

A census of oceanic anticyclonic eddies in the Gulf of Alaska

Stephanie A. Henson*, Andrew C. Thomas

School of Marine Sciences, University of Maine, Orono, ME 04469, USA

Received 17 May 2007; received in revised form 15 November 2007; accepted 26 November 2007
Available online 3 December 2007

Abstract

In the Gulf of Alaska (GOA), mesoscale eddies play an important role in promoting off-shelf transport of heat, nutrients and biological populations into the HNLC water of the northeast Pacific Ocean. However, the spatial and temporal distribution of these eddies and their characteristics have not been substantially described. Here we apply an objective method (Okubo–Weiss parameter) for identifying and tracking eddies to 15 years (October 1992–2006) of satellite sea level anomaly data. The parameter allows the spatial and temporal variability in eddy activity to be defined, providing the first systematic census of anticyclonic eddies in the region. Eddies are generated principally on the eastern side of the basin and propagate either westward (Haida eddies) or along the western GOA shelf break (Alaskan Stream eddies). Seasonal maps of eddy density show fewest eddies in winter, maximum in spring/summer. The Haida and Alaskan Stream eddy corridors are clearly defined, as is an ‘eddy desert’ in the southwest of the basin, where the probability of an eddy being identified is zero. Maps of eddy trajectories for each year show substantial interannual variability in number and propagation paths. Greatest eddy activity occurs in 1994, 1997/1998 and 2004. Fewest eddies occur in 1996 and in the period from 1999 through 2002. Interannual variability in eddy characteristics (magnitude, propagation speed, diameter and duration) is assessed for the basin as a whole, and separately for the Alaskan Stream, Haida and Sitka/Yakutat formation regions. In general, Alaskan Stream eddies are more numerous, larger and more intense than Haida eddies. Periods of increased eddy activity do not necessarily correspond to El Niño events, but are associated with anomalous downwelling wind conditions along the continental margin.

© 2007 Elsevier Ltd. All rights reserved.

Keywords: Mesoscale eddies; North Pacific Ocean; Alaskan Gyre; ENSO; Interannual variability

1. Introduction

The Gulf of Alaska (GOA) is a highly productive region, despite the predominantly downwelling conditions experienced year-round. The circulation is dominated by a wind-forced gyre in the ocean basin whose southern boundary is the North Pacific

Current, which splits as it approaches the North American continent into the equatorward California Current and the poleward Alaska Current (Fig. 1). The Alaska Current turns south-westward at the head of the Gulf, and becomes a narrow, swift stream which closely follows the shelf break (from near Prince William Sound westward the current is named the Alaskan Stream). A portion of the Alaskan Stream turns southward again near the Aleutian Islands and recirculates as part of the North Pacific Current, closing the loop of the Alaska Gyre (Reed and Schumacher, 1986).

*Corresponding author. Present address: Atmospheric and Oceanic Sciences Program, Princeton University, Princeton, NJ 08540, USA. Tel.: +609 258 0979.

E-mail address: shenson@princeton.edu (S.A. Henson).

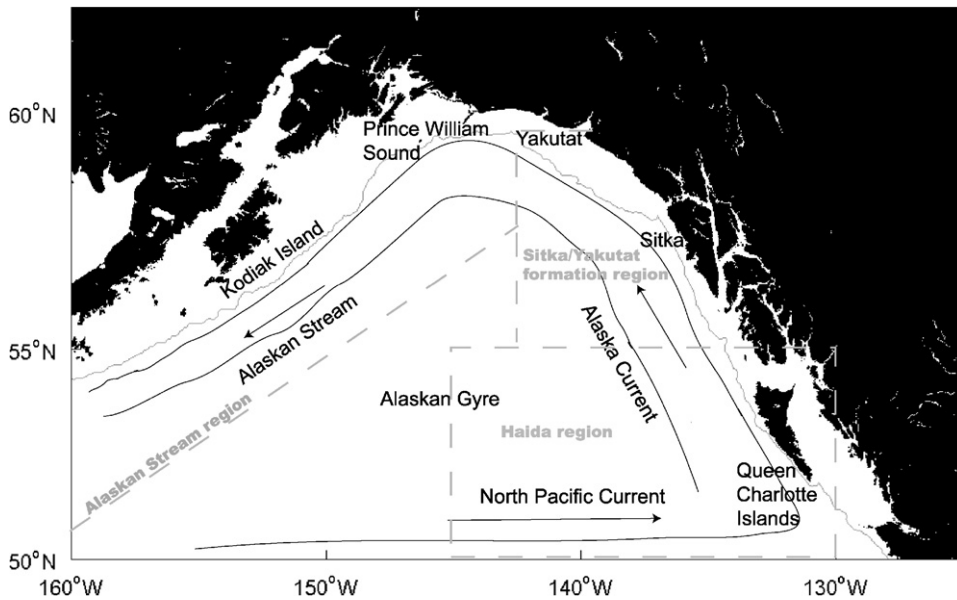


Fig. 1. Map of the study region with a schematic of principal currents and place names mentioned in text. Grey line is 500 m isobath; dashed grey lines mark approximate boundaries of Alaskan Stream, Haida and Sitka/Yakutat formation regions.

In situ surveys of GOA eddies find eddy cores several hundred to ~1500 m deep, containing warm, fresh, high nutrient water, compared to surrounding waters (e.g. Crawford, 2002; Ladd et al., 2005a; Peterson et al., 2005; Whitney and Robert, 2002). Although high chlorophyll concentrations are evident on the shelf, offshore of the shelf break high nutrient-low chlorophyll (HNLC) conditions prevail and phytoplankton growth is believed to be iron limited (Martin and Fitzwater, 1988; Boyd et al., 2004). The cross-shelf exchange of macronutrients, iron and phytoplankton and zooplankton populations are enhanced by mesoscale eddies propagating along the shelf break (e.g. Stabeno et al., 2004; Johnson et al., 2005; Okkonen et al., 2003; Mackas and Galbraith, 2002). Satellite ocean colour images confirm that eddies draw high chlorophyll water off the shelf, increasing productivity and transport of carbon into the interior of the Gulf (Crawford et al., 2002, 2005; Okkonen et al., 2003). Crawford et al. (2007) suggest that these eddies play a significant role in controlling the time and space patterns of chlorophyll in the GOA, and may therefore determine the biological productivity and ecological function of the region.

On the basis of their formation location, three groups of eddies (all predominantly anticyclonic) are commonly recognised in the GOA: Haida, Sitka and Yakutat eddies. Haida eddies are usually generated near the southern tip of the Queen

Charlotte Islands (Fig. 1). First observed in drogued drifter tracks by Kirwan et al. (1978), the eddies may be generated as a result of warm, fresh water advected out of Hecate Strait (Di Lorenzo et al., 2005). These buoyant plumes generate a series of small eddies, which may merge to form a larger eddy. Once shed from the island, Haida eddies propagate westward, carrying with them water and organisms representative of coastal conditions (Crawford, 2005; Batten and Crawford, 2005).

A second group of eddies form near Sitka, Alaska. Before the advent of satellite altimetry, Tabata (1982) catalogued oceanographic data collected near Sitka, concluding that recurring anticyclonic eddies are generated in this region. Reversals of downwelling winds, atmospherically forced planetary waves, or the interaction of the Alaskan Current with topography have all been suggested as possible formation mechanisms (Thomson and Gower, 1998; Willmott and Mysak, 1980; Swaters and Mysak, 1985). Sitka eddies have been observed to propagate either westward (Gower, 1989; Matthews et al., 1992), or towards the northwest, becoming embedded in the Alaskan Stream (Crawford et al., 2000). Satellite ocean colour data shows that high chlorophyll waters are also drawn off the shelf by Sitka eddies (Crawford et al., 2005).

The final group of eddies form near Yakutat, Alaska. Generation mechanisms are likely to be similar to those for Sitka eddies. Yakutat eddies

propagate first northwestward, then turn southwestward with the Alaskan Stream and closely follow the isobaths (e.g. Ladd et al., 2007). The eddies tend to stay very close to the shelf break (within ~200 km) throughout their lives. *In situ* data show that the Yakutat eddies' water properties closely resemble those of shelf water, suggesting that cross-shelf exchange of material occurs subsequent to eddy formation (Okkonen et al., 2003; Ladd et al., 2005a, b). SeaWiFS ocean colour data show filaments of high chlorophyll are transported off the shelf, wrapping around the outer edge of the eddy (Okkonen et al., 2003; Ladd et al., 2005a; Crawford et al., 2007).

Assessment of early altimetry data demonstrated that eddies could be identified in sea level anomaly (SLA) data, and that interannual variability in eddy activity does occur in the GOA (Crawford and Whitney, 1999; Crawford, 2002; Okkonen et al., 2003). In the first GOA-wide assessment of multi-instrument SLA data, Ladd (2007) used the distribution of eddy kinetic energy to investigate the interannual and spatial variability in mesoscale activity. We expand on her study, applying an objective eddy identification algorithm to 15 years of SLA data. Our goal is to conduct an eddy census that systematically quantifies the number, location, size and speed of eddies, and their spatial, seasonal and interannual variability. Preliminary results concerning the forcing patterns that may contribute to the observed interannual variability are discussed.

2. Methods

The Okubo–Weiss parameter (Okubo, 1970; Weiss, 1991) aims to separate a velocity field into regions of high vorticity and high strain. The parameter has been successfully applied to SLA images from the Mediterranean Sea (Isern-Fontanet et al., 2003, 2004, 2006), the Tasman Sea (Waugh et al., 2006) and globally (Chelton et al., 2007). Here, we apply the Okubo–Weiss parameter to a 15-year time series of SLA to determine the spatial and temporal distribution of mesoscale eddies in the GOA. Multi-mission, merged, mapped SLA data from October 1992 to December 2006 were obtained from <http://www.avisioceanobs.com>. The dataset consists of merged data from ERS, Envisat (both European Space Agency missions), Topex/Poseidon and Jason-1 (NASA/CNES joint projects) instruments. Using multiple instruments allows reduced

errors and increased resolution, i.e. 7-day, 0.25° in both latitude and longitude (Le Traon et al., 2003; Pascual et al., 2006). Comparisons of *in situ* and altimetric estimates of sea-surface height within Haida eddies suggest that, because of satellite track separation and contouring algorithms, the satellite data underestimate eddy height by a few centimetres (1–6 cm; Yelland and Crawford, 2005). SLA data obtained near shore are unreliable, and measurements made over water depths shallower than 500 m were excluded from the analysis. The spatial mean was removed from each weekly SLA map to compensate for seasonal steric effects.

The velocity field was derived from SLA, h , assuming geostrophy:

$$u = -\frac{g}{f} \frac{\partial h}{\partial y}, \quad v = \frac{g}{f} \frac{\partial h}{\partial x}. \quad (1)$$

An eddy, by definition, will consist of a region of high vorticity (eddy core), surrounded by a circulation cell, which experiences high rates of strain. Vorticity (ω) and the normal (s_n) and shear (s_s) components of the strain are defined respectively as:

$$\omega = \frac{\partial v}{\partial x} - \frac{\partial u}{\partial y}, \quad s_n = \frac{\partial u}{\partial x} - \frac{\partial v}{\partial y}, \quad s_s = \frac{\partial v}{\partial x} + \frac{\partial u}{\partial y}. \quad (2)$$

The Okubo–Weiss parameter, W , combines these terms:

$$W = s_n^2 + s_s^2 - \omega^2, \quad (3)$$

so that the sign of W allows determination of regions that are either strain-dominated ($W > 0$) or vorticity-dominated ($W < 0$).

Eddy cores appear as coherent regions of negative W (for both cyclonic and anti-cyclonic eddies) against a background field of small positive and negative W values. (We define an eddy core as a coherent region of high vorticity; the terminology is not intended to imply an association with the anomalous sub-surface waters of an eddy.) In keeping with previous studies (e.g. Pasquero et al., 2001; Isern-Fontanet et al., 2006), we define the eddy core threshold value of W as $-0.2\sigma_w$, where σ_w is the standard deviation of W , calculated at each weekly time step, in the entire region, in this case the GOA region defined in Fig. 1 (50–62°N, 160–125°W). For each weekly SLA field, W was calculated at every pixel location. Because eddies in the GOA are almost exclusively anti-cyclonic, we only retained groups of pixels identified as eddy cores that encompassed entirely positive SLA. No lower limit on the eddy height was set; i.e. every

pixel identified as ‘eddy’, provided $SLA > 0$, was retained. Operation of the Okubo–Weiss parameter is illustrated in a transect of W and SLA across a Haida eddy on 18 June 2000 (Fig. 2). Large negative values of W typify the eddy core, with smaller, positive W in the strain-dominated rings of the eddy. We use only the pixels identified as eddy core in all subsequent analyses. Note that this results in an underestimate of the total diameter of an eddy (Fig. 2). Visual examination of many W transects suggests that the diameter of the eddy core is ~ 50 – 60% of the total eddy diameter.

To track individual eddies in time we use a pixel connectivity algorithm, which identifies groups of pixels that are adjacent in directions x and y , and in time. For each weekly SLA map, pixels identified as eddy core are assigned a value of 1, whilst all other

pixels are given a value of 0. At each time-step, at each pixel identified as ‘eddy’, the algorithm searches for any adjacent pixels (in x , y and time) that also have a value of 1. Groups of connected pixels are assigned a unique identifying number (unique, and also not 1 or 0), and the algorithm then moves on to the next pixel with a value of 1, and repeats the search for adjacent pixels labelled 1. This criterion works well in the GOA, where eddies tend to be very coherent and well separated spatially from each other. More complicated tracking algorithms, based on the geometrical distance from one eddy centre to another, have also been successfully employed (e.g. Isern-Fontanet et al., 2006). The principle weakness of this tracking method is that if an eddy weakens for one time-step (either because it genuinely weakens, or because it falls between satellite tracks) so that its vorticity drops below the threshold value of W , but then strengthens again, it will be identified as two separate eddies. If an eddy splits, or two eddies merge, these will also be identified as separate eddies. In the final processing step, any small eddies with cores less than nine pixels in size (\sim equivalent to a diameter of 80 km) or short-lived features with duration < 12 weeks were discarded.

In total 129 anticyclonic eddies that met our criteria were identified in the 14-year time series (1993–2006). The eddy tracking was also repeated for cyclonic eddies ($W < -0.2\sigma_w$ and $SLA < 0$). A total of 23 cyclonic eddies were identified (i.e. $\sim 15\%$ of all eddies) and were found to be short-lived (on average 17 weeks, compared to 33 weeks for the anticyclonic eddies) and weak (average magnitude of -8 cm, compared to 27 cm for anticyclonic eddies). Because of the dominance of anticyclonic eddies, they will be our focus in the remainder of the paper. The reader is reminded that because of the criteria we have set for tracking eddies only large (> 80 km diameter) and long-lived (> 12 weeks) eddies are included in our analysis.

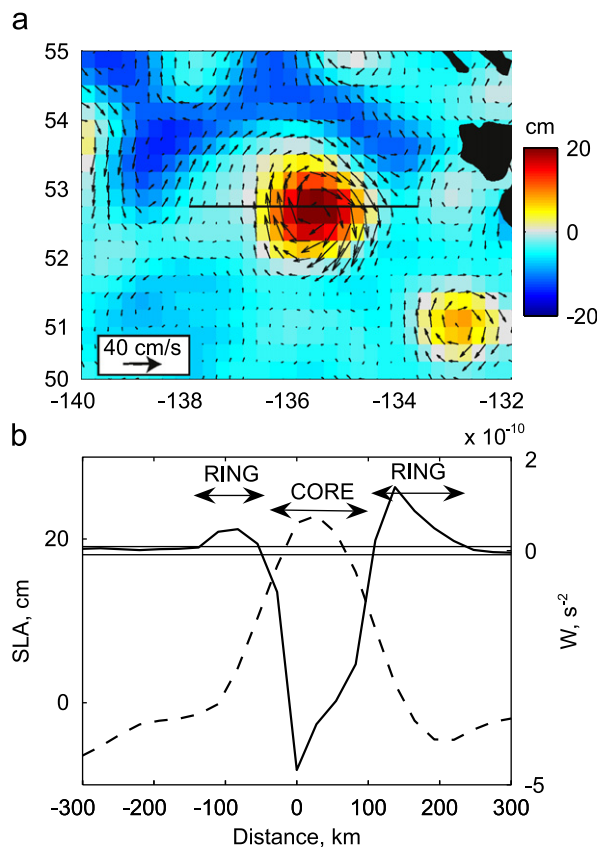


Fig. 2. Illustration of the Okubo–Weiss parameter in a transect across a Haida eddy on 18 June 2000. (a) SLA (cm) overlaid with geostrophic velocity anomaly vectors (cm s^{-1}). Horizontal line marks position of transect shown in (b). SLA (dashed line) and Okubo–Weiss parameter (solid line) plotted as function of distance from centre of the eddy. The eddy core and rings, defined as $W < -0.2\sigma_w$ and $W > 0.2\sigma_w$ (horizontal lines), respectively, are marked.

3. Results

3.1. Eddy identification

To illustrate the performance of the Okubo–Weiss parameter, a series of SLA maps (at \sim monthly intervals) from 2000 are plotted in Fig. 3. Overlaid are the locations of the eddy cores as identified using the criteria outlined in the Methods section. The eddy cores in this figure are, on average, ~ 100 km in

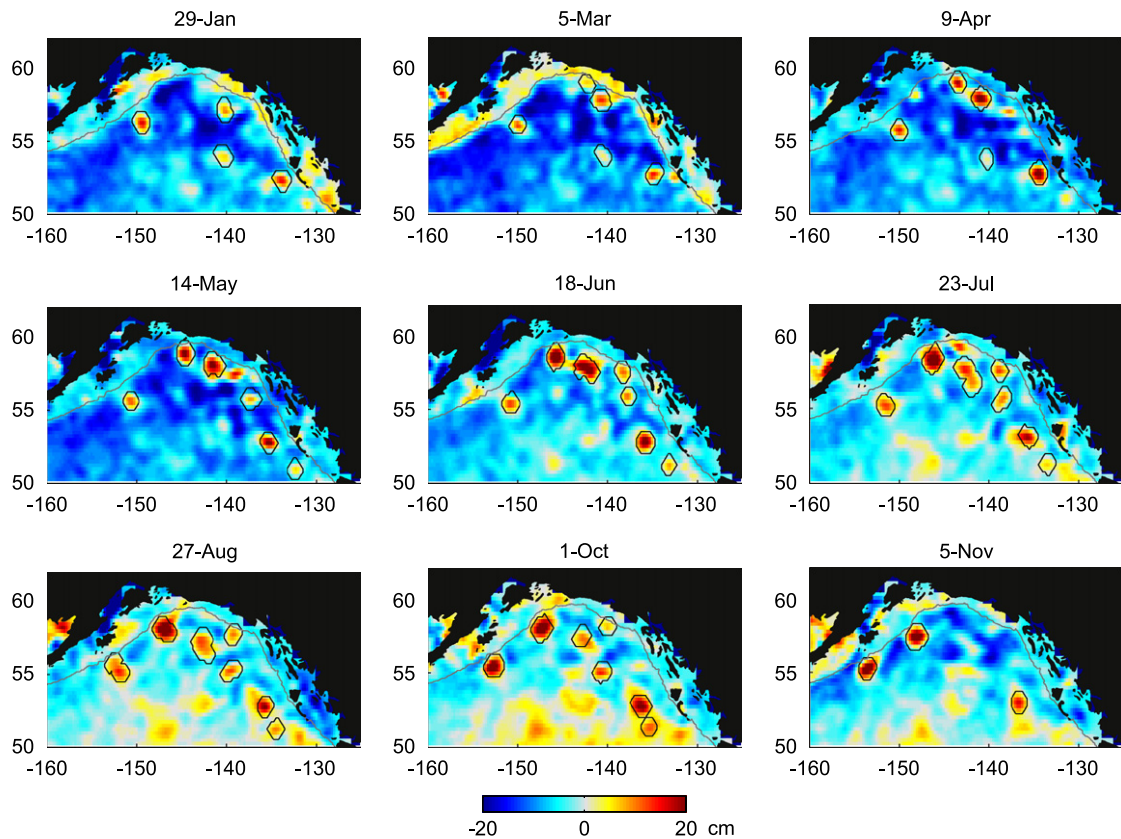


Fig. 3. Example of weekly sea level anomaly fields for 2000. Black lines denote anticyclonic eddy cores identified by the Okubo–Weiss parameter. Grey lines mark 500 m isobath.

diameter, with the largest at ~ 155 km. In January 2000 four eddies existed in the GOA, one located near the Queen Charlotte Islands (QCI), one west of QCI (which originated at QCI ~ 3 months earlier), one northwest of Sitka and one propagating along the shelf break near Kodiak Island. In March and April, an additional eddy located near Yakutat was evident. The number of eddies in the region peaked at seven in June–October. In August 2000, a string of eddies stretched northwest from southern QCI to Yakutat, spaced ~ 300 km apart. Along the western shelf, there are two eddies propagating parallel to the shelf break, ~ 450 km apart and moving at ~ 2 km day $^{-1}$. In November 2000, eddy activity receded again, leaving just three eddies in the basin.

The images in Fig. 3 are for 2000, but are typical of the mesoscale conditions in the GOA. Overall, the method performs well, successfully locating eddy cores. Occasionally, two neighbouring eddy cores are identified, where the naked eye would suggest only one large eddy, or a feature that is not classed as an eddy appears (likely because it is too

small, or is short-lived). However, after visual examination of a large number of such plots we are satisfied that eddies are being correctly classified, and moreover, the Okubo–Weiss parameter provides an objective, and physically based, method of eddy identification.

3.2. Eddy trajectories

The ability of this method to track eddies in time is demonstrated in Fig. 4, where the trajectories of individual eddy centres for each year are plotted. The eddy centres are calculated as the geometrical mean of the pixels within each individual eddy core. Trajectories are computed by joining adjacent centres at 7-day intervals. Tracks of eddies that persist from 1 year to the next are marked with matching symbols, to assist in following an eddy over the course of its lifetime. Note that shallow regions (depth < 500 m) are excluded from the analysis, and therefore no conclusion can be drawn on whether eddies exist on the shelf. In the majority

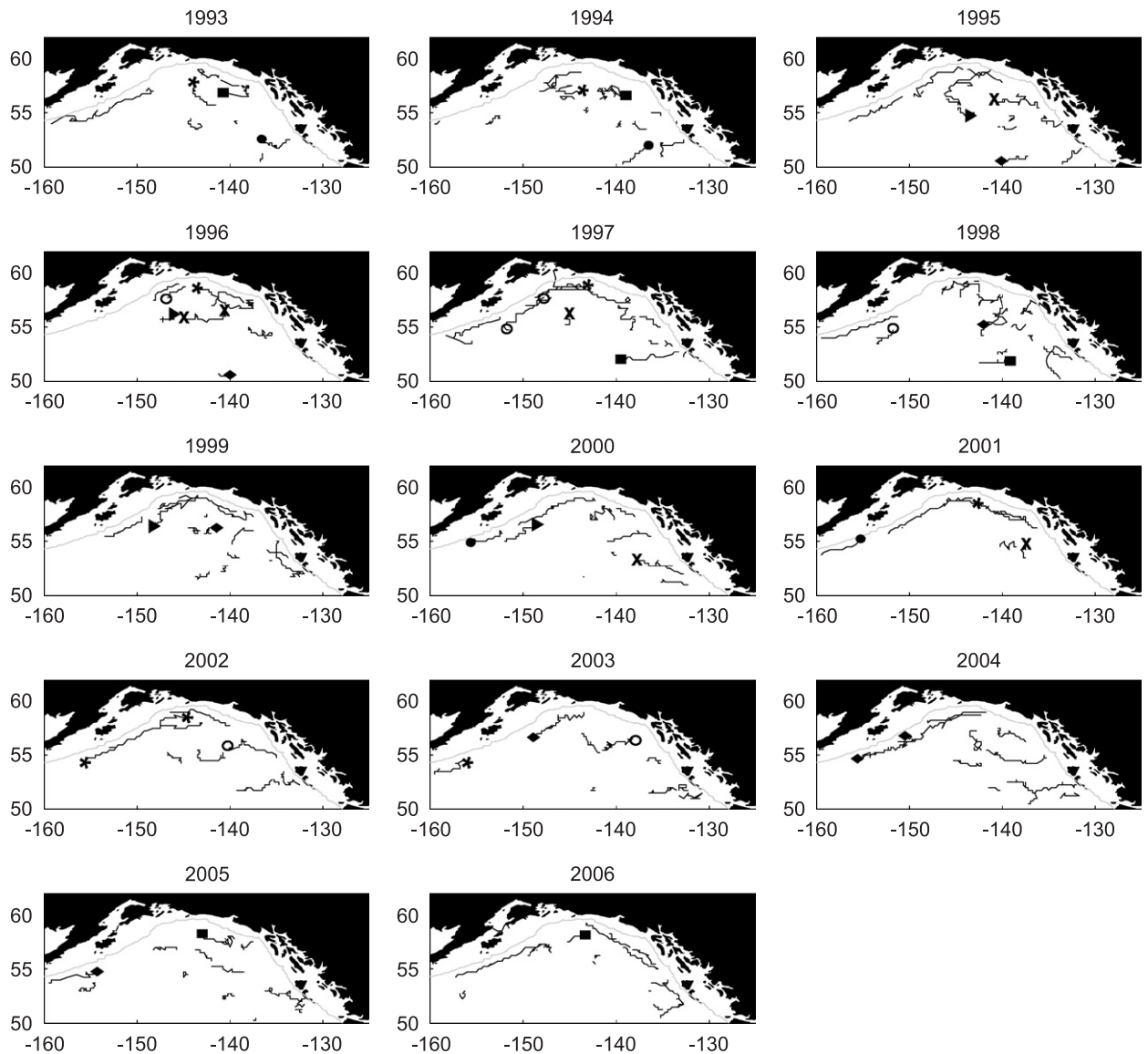


Fig. 4. Interannual variability in trajectories of anticyclonic eddies over the study period 1993–2006. For eddies that persist longer than 1 year, the end location in their first year and start location in their second year are marked with matching symbols. Grey lines mark 500 m isobath.

of years, 1–2 Haida eddies and a similar number of Sitka eddies are generated and propagate westward. Almost every year, 1–2 Yakutat eddies are also formed and propagate westward around the Gulf, following the isobaths closely. However, no clear distinction is apparent between the Sitka and Yakutat formation regions. Eddies generated near the coast anywhere between ~ 55 and 58°N may propagate either westward or parallel to the isobaths. To avoid confusion, in the remainder of the paper, ‘Yakutat eddies’ will be used to refer to

any eddy that becomes entrained in the Alaskan Stream and propagates southwestward parallel to the shelf break, regardless of whether it was generated near Yakutat or farther south near Sitka.

Overall, the eddy tracks are consistent both with our visual examination of the SLA data and with previous studies of eddies in this region, which have been investigated by visually tracking eddies in individual SLA images (Crawford and Whitney, 1999; Crawford, 2002) or by plotting specific contours of SLA (e.g. 25 cm in Ladd, 2007). Our

results show some of the same features, e.g. the southward movement of Haida eddies in 1995 and 1998, but also display differences in paths of specific eddies. The Okubo–Weiss parameter identifies eddies on the basis of their vorticity characteristics and does not require us to impose a lower limit on the magnitude of the eddies we track. Therefore, more eddies are identified in our analysis than on the basis of contouring a particular SLA height (e.g. Crawford, 2002; Ladd, 2007). There is considerable interannual variability in the number of eddies and their tracks. This is discussed in detail in the following section.

The spatial and seasonal distribution of eddies in the GOA is not uniform. Fig. 5a shows the climatological spatial distribution of eddies, plotted as the percentage of weeks in which each pixel was flagged as ‘eddy’ for the entire time series. The climatological seasonal patterns are shown in

Figs. 5b–e (winter is December–February, etc.). Overall, eddies occur most frequently (~15% of the time) in a small patch just west of QCI (~132°W, 53°N), in an area west of Sitka extending westward into the basin (~56–58°N), and in a band stretching from west of Sitka, northwest around the head of the Gulf and along the shelf break past Kodiak Island. Offshore of QCI, eddy probability is ~8% in a large patch at ~50–53°N, 130–140°W representing the tracks of westward propagating Haida eddies. The tracks of westward propagating Sitka eddies appear as an extensive region of moderately high eddy probability (~10%) occurring between ~55–57°N, 140–145°W. From ~145 to 155°W a narrow band of high eddy probability (~12%) closely follows the shelf break highlighting the Yakutat eddy tracks. At the head of the Gulf this eddy corridor is ~180 km wide and becomes wider further west, expanding to ~300 km wide at 155°W.

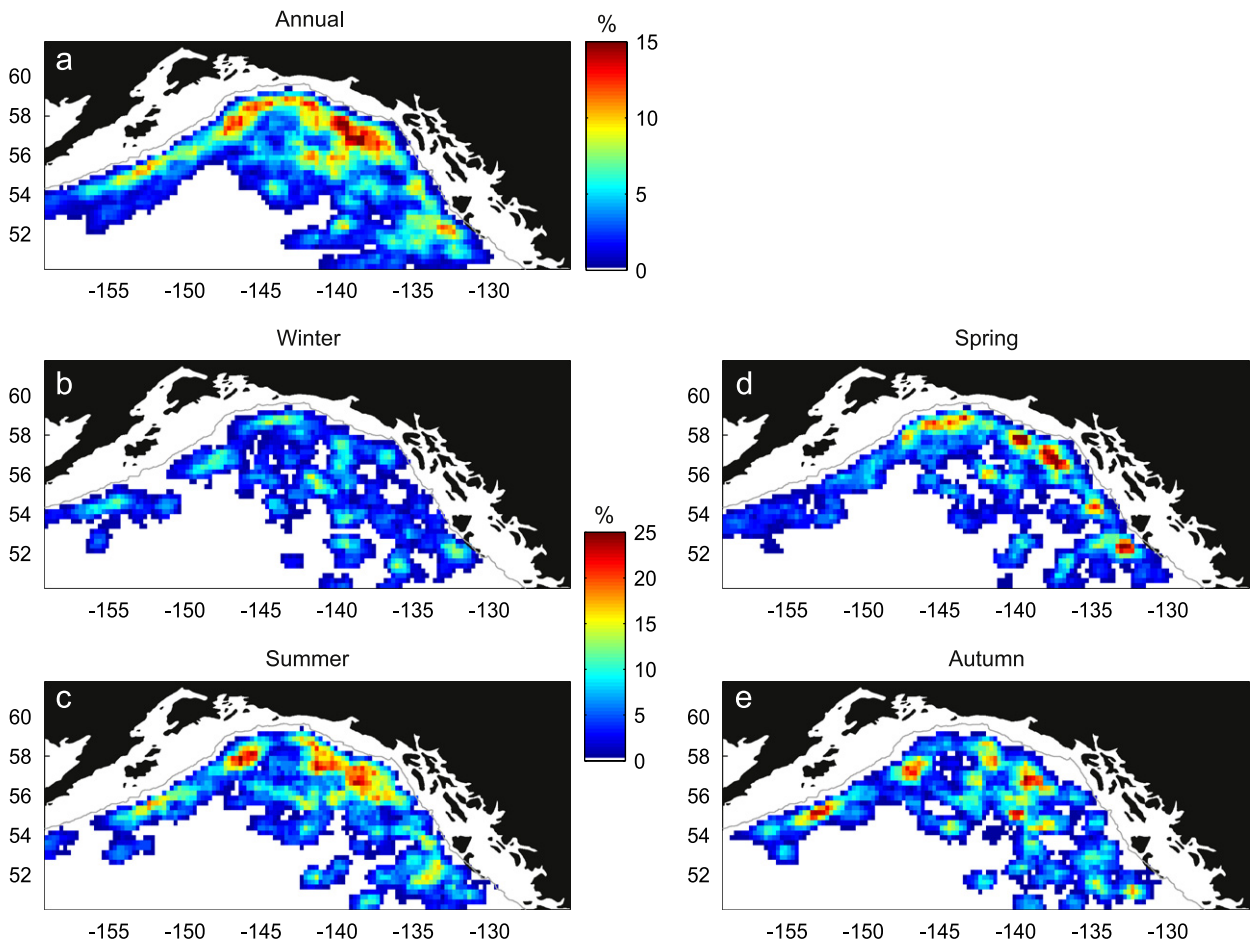


Fig. 5. Climatological spatial patterns of eddy occurrence, quantified as the probability, at each pixel, of an eddy occurring over (a) the entire time series and (b–e) in each season (winter is December–February, etc.).

West of Kodiak Island eddy probability declines. This is likely because eddies reaching the edge of the domain become truncated and so are excluded from the analysis as they appear to be too small. West of $\sim 145^\circ\text{W}$, south of the Yakutat eddy corridor, eddy probability is close to zero. This region is sufficiently far from the eddy-generating coastal areas of Haida and Sitka that westward propagating eddies decay before reaching it. Yakutat eddies propagate parallel to the isobaths and also do not enter this 'eddy desert'.

Eddy kinetic energy (EKE) is expected to have a similar distribution as eddy probability, and indeed Ladd's (2007; her Fig. 1) map of mean EKE shows many similarities to Fig. 5 and allows us to confirm, via another method, some of the features we have identified. High EKE occurs off QCI, in a broad region extending from Sitka around the head of the Gulf to near the Kenai Peninsula, and in a tight band along the shelf break at least as far as Unimak Pass (54.2°N , 164.5°W). Ladd's (2007) study region extends further west than ours, showing high EKE extending along the shelf break well beyond Kodiak Island. The drop in eddy probability at the edge of our study region is therefore likely due to eddies being truncated, rather than a lack of eddies propagating beyond Kodiak Island. A region of extremely low EKE is also evident in Ladd (2007), which coincides with our 'eddy desert'. Although small, short-lived eddies, which escape detection by our criteria, may exist here, the very low EKE suggests that eddies are indeed a rare occurrence in this region. A global analysis of eddy trajectories, conducted using the Okubo–Weiss method, also clearly shows the continuing propagation of eddies past Kodiak Island and the existence of an eddy desert in the offshore Northeast Pacific (Chelton et al., 2007).

In Figs. 5b–e, eddy probability is plotted separately for each season. Similar spatial patterns of eddy distribution exist in all seasons, but the probability varies from a minimum of 2–10% in winter to greater than 25% in some areas in spring. The majority of eddies are observed in spring and have either propagated out of the region or decayed by winter. The seasonal progression of Yakutat eddies along the shelf break is especially clear. In spring, maximum eddy probability occurs in a band from ~ 135 to 148°W along the shelf break. By summer, high eddy density extends throughout the eddy corridor from near Sitka to west of Kodiak Island. The highest eddy probability is located

southwest of Kodiak in autumn, and the eddy corridor no longer extends continuously back to Sitka. In winter, only small patches of eddy probability greater than zero exist along the shelf break.

GOA eddies are generally thought to be generated in winter, when downwelling winds are at a maximum (e.g. Tabata, 1982). Our results suggest however that more eddies exist in spring (March–May) than in any other season. Other studies conducted using SLA data have noted that the maximum EKE or eddy area occurs in March (Ladd, 2007) or 'late winter' (Crawford, 2002). The exclusion of shelf data and eddies smaller than ~ 80 km in diameter in our analysis makes it unlikely that the actual moment of generation or formation of eddies is captured in our results. Instead, eddies are not identified until they have detached from the shelf.

3.3. Interannual variability

There are distinct interannual differences in frequency and trajectories of eddies in the GOA (Fig. 4). An obvious example is the scarcity of Yakutat eddies propagating along the shelf break in 1994, 1996 and 2005. There are also years when Haida eddies are scarce, such as 1996 and 2001. (Although note that a Haida eddy was present in 2001 (Miller et al., 2005 and other papers in that volume) but was too small to meet our criteria.) In some years, the eddy tracks are distinct, e.g. the Haida and Sitka eddies in 2002, or the train of Yakutat eddies in 2001 which have long tracks parallel to the shelf break. In other years the eddy corridors are less well defined and the eddy field is composed of disjointed tracks that do not form coherent trajectories (e.g. 1994 and 2005).

One quantitative measure of eddy activity is the total area in each weekly SSH image identified as 'eddy core'. The total for the entire study region is presented in Fig. 6a as an anomaly from the climatological mean. The mean area covered by eddy cores is $\sim 89,000$ km², equivalent to $\sim 4\%$ of the study region. Eddy area peaks in 1994, 1998 and 2004, with minima in 1996 and 1999 through 2002. Interannual variability in the eddy core area, separated into Alaskan Stream, Haida and Sitka/Yakutat formation regions, is shown in Fig. 6b. (The geographical locations of the regions are plotted in Fig. 1.) In the Haida region increased eddy area occurs in 1994/1995, 1998 and 2004/2005,

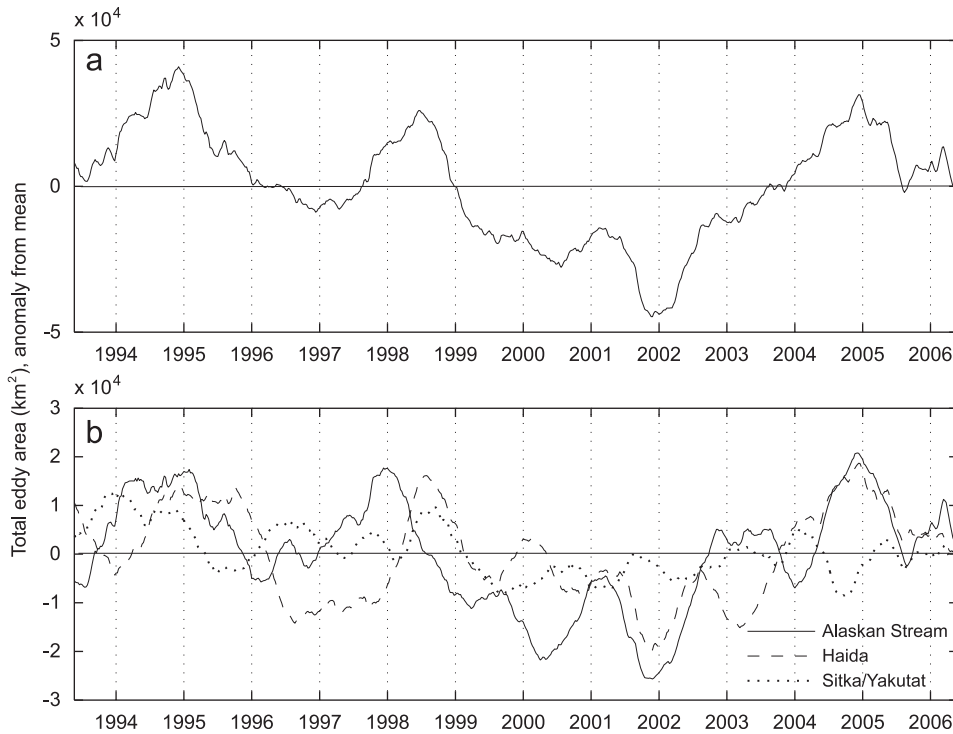


Fig. 6. Time series of total eddy core area (km^2) in each weekly SLA field, presented as an anomaly from the climatological mean, for (a) the entire Gulf of Alaska region and (b) for the Alaskan Stream, Haida and Sitka/Yakutat formation regions (see Fig. 1 for locations). Mean area covered by eddy cores is $\sim 89,000 \text{ km}^2$ ($\approx 4\%$ of the study region). Time series has been truncated to exclude end effects of the method (eddies' lifespans are artificially curtailed). Year labels indicate 1 January.

whereas 1996/1997 and 2001–2003 have fewer than average eddies. The eddy area in the Alaskan Stream region is similar with peaks in 1994, 1997/1998 and 2004, and a sustained minimum from 1999 to 2002. In the Sitka/Yakutat formation region, eddy area is less variable than in the other 2 regions, although small peaks do occur in 1994 and 1998. However, unlike in the other regions, eddy area in the Sitka/Yakutat formation region is below the mean in 2004. Interestingly, the 1997/1998 peak occurs earlier in the Alaskan Stream area than in either the Haida or Sitka/Yakutat regions. However, the 2002 minimum and the 2004 peak occur at the same time in both the Alaskan Stream and Haida regions.

Ladd (2007) calculated interannual variability in EKE in three areas of the GOA, which, although smaller, approximate our three regions. Because of the differences in areas used and because the EKE and eddy area are two different measures of mesoscale activity, our results are not directly comparable with Ladd's (2007). Despite this, it is encouraging to note that distinct similarities do occur, such as the minimum in 2001 and maximum

in 2004 in the Haida region. Crawford (2002) calculated eddy area (as defined by the area enclosed by SLA contours of 10 cm) in the eastern GOA from 1993 to mid-2001. His region encompasses both our Haida and Sitka/Yakutat formation regions, so again the datasets are not directly comparable; however, both time series show peaks in 1995 and 1998.

Another quantitative measure of eddy activity is a simple count of the number of eddies and their properties. Interannual variability in eddy frequency is summarised in Fig. 7 as the number of individual eddies identified in each year, and their magnitude and propagation speed, as an anomaly from the climatological mean. On average, 13 eddies occur each year in the GOA. Of these, 5.5 occur in the Haida, 6 in the Alaskan Stream and 3.5 in the Sitka/Yakutat formation region. Fewer eddies than usual are identified in the GOA in 1993, 1996 and 2000–2003 (Fig. 7a). Generally, the Haida and Alaskan Stream regions show the same pattern of maxima and minima as for the entire GOA (Figs. 7b and c). The Sitka/Yakutat formation region, however, differs slightly, with minima occurring in

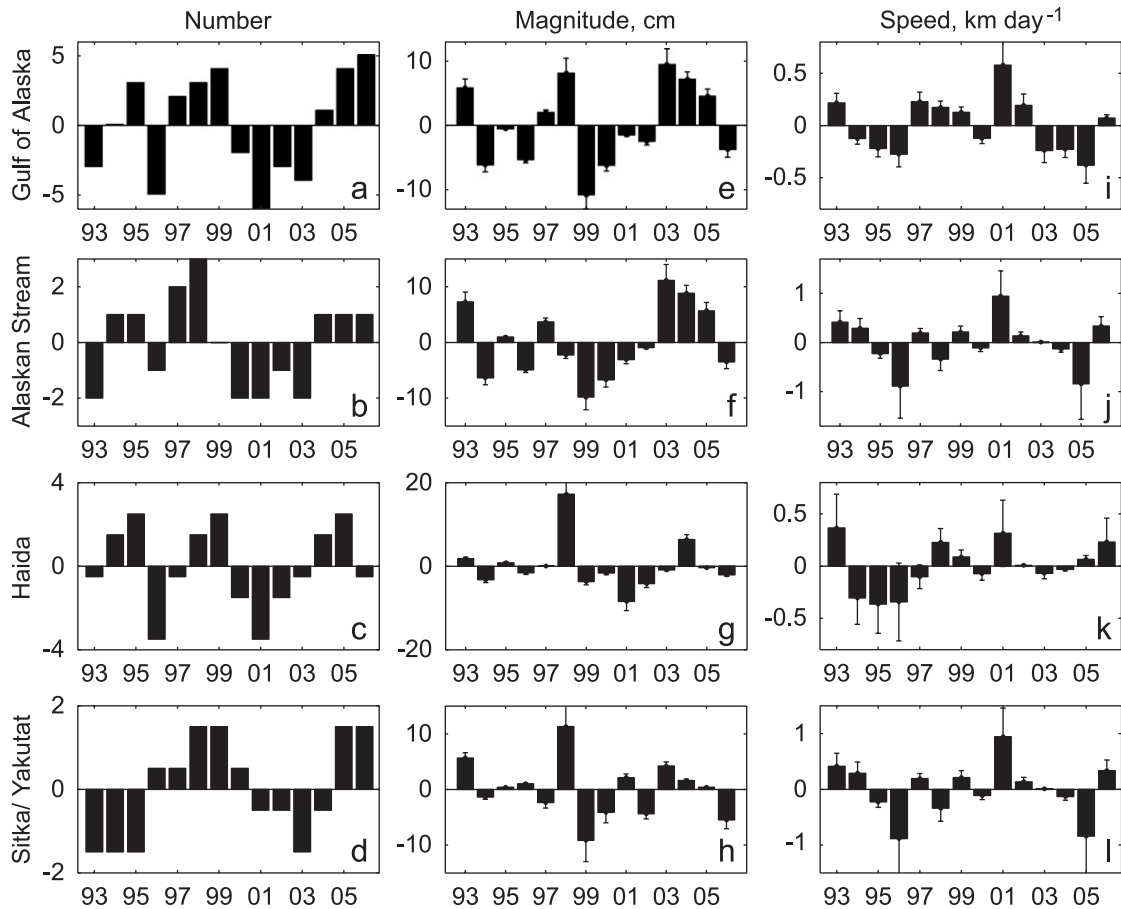


Fig. 7. Annual mean eddy characteristics, presented as anomaly from the mean (mean values are in Table 1) for the entire Gulf of Alaska, Alaskan Stream, Haida and Sitka/Yakutat formation regions: (a–d) number of individual eddies identified in each year, (e–h) magnitude of eddies (cm), and (i–l) propagation speed of eddies (km day^{-1}). Whiskers on bars indicate the standard deviation.

1993–1995 and 2001–2004 (Fig. 7d). The magnitude of the eddies is calculated as the maximum SLA within each eddy core. The years with most eddies do not necessarily have the strongest eddies. For example, in 2003 there were fewer than average eddies, but they were very intense; and the opposite is true for 1999 (Fig. 7e). Unusually strong eddies occurred in 1998 in both the Haida and Sitka/Yakutat formation regions (Figs. 7g and h; also noted by Crawford, 2002). Eddy propagation speeds average 2.4 km day^{-1} , with fastest eddies occurring in 2001 in all regions (Figs. 7i–l). This is also the year that consistently has fewest eddies. Generally, fast eddies have long tracks, propagating close to the shelf break in the western GOA. Conversely, years with slow propagation speeds tend to be those that exhibit disjointed eddy tracks, such as 1996 and 2005. A similar finding was reported by Okkonen et al. (2003), who concluded

that trajectories of fast propagating eddies lie closer to the shelf break than those of slower eddies.

Table 1 summarises mean eddy properties for the entire GOA, and separately for each of the 3 sub-regions. Eddies occur more frequently in the Alaskan Stream and Haida regions (6 and 5.5 eddies per year) than in the Sitka/Yakutat formation region (3.5 eddies per year). The magnitude of the eddies is on average $\sim 27 \text{ cm}$. Alaskan Stream eddies are more intense than either the Haida or Sitka/Yakutat eddies (mean magnitude of 25.5 cm versus 18–19 cm). Eddies also propagate somewhat faster in the Alaskan Stream and Sitka/Yakutat regions than in the Haida region (2.0 km day^{-1} versus 2.5 km day^{-1}). The mean eddy core diameter is $\sim 114 \text{ km}$ (estimated assuming a radially symmetrical eddy core). Eddies are slightly smaller, on average, in the Haida than the Alaskan Stream and Sitka/Yakutat regions (97 versus 108–110 km

Table 1
Mean eddy characteristics for the entire Gulf of Alaska and for the Alaskan Stream, Haida and Sitka/Yakutat formation regions

	Gulf of Alaska	Alaskan Stream	Haida	Sitka/Yakutat formation
Number of eddies (year ⁻¹)	13 (7, 18)	6 (4, 9)	5.5 (2, 8)	3.5 (2, 5)
Magnitude (cm)	27.3 (10.5, 53.4)	25.5 (6.2, 53.4)	17.9 (3.9, 52.4)	19.3 (2.5, 49.2)
Propagation speed (km day ⁻¹)	2.4 (0.38, 4.5)	2.5 (0.46, 4.5)	2.0 (0.46, 2.9)	2.45 (0.38, 3.25)
Core diameter (km) ^a	104 (82, 225)	108 (82, 189)	97 (82, 148)	110 (82, 225)
Duration (weeks) ^b	33 (13, 131)	30 (13, 130)	30 (13, 76)	31 (13, 115)

Minimum and maximum values are in brackets.

^aOnly eddies with diameters greater than ~80 km included in analysis.

^bOnly eddies which persist for greater than 12 weeks included in analysis.

diameter). This difference could be due to the more northerly formation region of the Yakutat and Sitka eddies and the associated decrease in Rossby radius (Stammer, 1997; Chelton et al., 2007); however, both the change in latitude and eddy size are too small to address this. The diameters reported in Table 1 are less than the ~150–200 km reported in previous papers (Musgrave et al., 1992; Crawford et al., 2000; Crawford, 2005), likely because the Okubo–Weiss method locates only the high-vorticity core of the eddy and excludes the outer, strain-dominated rings (Fig. 2). The average duration of an eddy is ~8 months, with the longest-lived eddies persisting for ~2.7 years (usually Alaskan Stream eddies). The longest-lived Haida eddy in comparison only persists for 1.5 years. These maximum durations are likely to be underestimates, as once an eddy propagates out of our study region or weakens so that it no longer meets our criteria, it is not tracked further. Crawford et al. (2000) suggest that Yakutat eddies can survive for up to 3 years, and Ladd et al. (2007) tracked one Yakutat eddy which persisted for more than 5 years.

4. Discussion

Pronounced interannual variability in the number of eddies generated each year is evident (Fig. 7a). It has been hypothesized that ENSO events impact GOA eddies via the excitation of coastal Kelvin waves, which propagate poleward from the tropics, triggering instabilities in the AC (Murray et al., 2001; Melsom et al., 1999). An alternative hypothesis is that local wind forcing is responsible. Increased poleward (downwelling favourable) wind stress, increased wind stress curl along the eastern boundary, and subsequent increase in AC transport and intensification of the cyclonic gyre generate more mesoscale eddies (Okkonen et al., 2001;

Melsom et al., 2003; Ladd, 2007). However, as these conditions often coincide with El Niño events, both mechanisms may play a role. La Niña conditions may also result in fewer eddies, although this effect is less obvious in the modelling studies (e.g. Melsom et al., 1999). Our results show peaks in eddy area in 1994 and 1997/1998 (Fig. 5a), which correspond to the strong El Niño events of those years. Although the El Niño event of 2004/2005 was relatively weak, the increase in eddy area is as great as for 1997/1998. A similar response to the mild 2002/2003 El Niño event is, however, not observed. The years 1999–2002, which have weaker than average eddy area, correspond to a prolonged period of La Niña conditions.

We do not observe a consistent correspondence between ENSO events and eddy activity, although some El Niño years do have more eddies (e.g. 1998), and some La Niña years do have fewer (e.g. 2001). The GOA response to El Niño events is complex, arising from both oceanic and atmospheric teleconnections, and is likely to vary from one event to the next (e.g. Emery and Hamilton, 1985). ENSO events have profound impacts on wind stress patterns over the GOA (Schwing et al., 2002), and although we find no direct correlation between ENSO events and eddy activity, we do, however, find evidence that wind stress may play a role. The mean winter (December–February) wind stress for the entire time series and for eddy-rich years (1994, 1995, 1998 and 2004) and eddy-poor years (1996, 2000, 2001 and 2002) is contrasted in Fig. 8 (data from NCEP/NCAR reanalysis <http://www.cdc.noaa.gov/>). Strong (poor) eddy years were selected on the basis of a consistent positive (negative) anomaly in both eddy area (Fig. 6a) and frequency (Fig. 7a). In the climatology (Fig. 8a), poleward alongshore winds dominate the eastern side of the gulf, with northeastward winds across the western

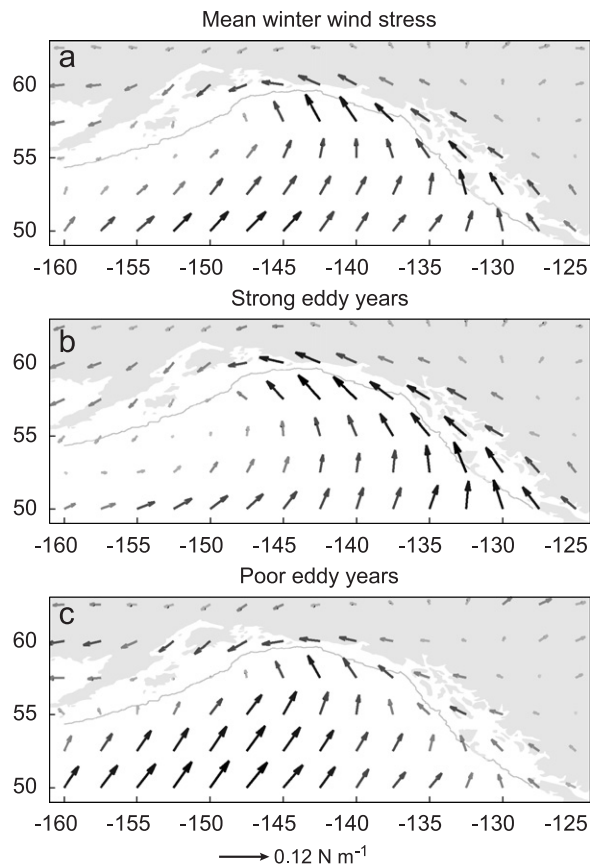


Fig. 8. Mean winter (December–February) wind stress for (a) entire time series 1992–2006, (b) eddy-rich years 1994, 1995, 1998 and 2004 and (c) eddy-poor years 1996, 2000, 2001 and 2002.

and central basin. In the years with elevated eddy activity (Fig. 8b) anomalously strong alongshore wind stress occurs in a band along the coast from south of QCI to Prince William Sound. Winds are poleward offshore of QCI, turning northwestward along the central Alaskan coast, i.e. winds are downwelling favourable along the entire stretch of eastern and central Alaskan coast. In eddy-poor years (Fig. 8c) wind stress is predominantly northeastward, with strongest winds occurring over the western basin. Winds are very weakly alongshore from QCI to Sitka and onshore at the shelf break from Yakutat to west of Kodiak Island. The implied Ekman transport is therefore eastward along the western and central Alaskan coast. In contrast, in the eddy-rich years the Ekman transport is onshore, implying an intensification of the AC. These results suggest that ENSO-mediated wind stress patterns are the dominant factor in controlling eddy activity. This is consistent with a recent modelling study that

concluded that interannual variability in wind forcing modulates the development of eddies, and that coastally trapped Kelvin waves are not necessary to eddy formation in the eastern GOA (Combes and di Lorenzo, 2007). We find that years of strong downwelling-favourable winds along the eastern shore of the basin correspond to years of increased eddy activity.

Interannual variability in the magnitude and tracks of the eddies will be important in the transport of water masses in the basin. The GOA eddies contribute greatly to the cross-shelf exchange of heat, salt, macronutrients and iron (e.g. Crawford et al., 2005; Peterson et al., 2005; Ladd et al., 2007; Johnson et al., 2005). In addition, enhanced chlorophyll concentrations in, and surrounding, eddies is frequently observed in satellite data (Okkonen et al., 2003; Ladd et al., 2005a; Crawford et al., 2005), and *in situ* sampling has demonstrated that on-shelf communities of phytoplankton and zooplankton are transported offshore by the eddies (Batten and Crawford, 2005; Mackas and Galbraith, 2002). The propagation of the eddies into the otherwise HNLC waters of the basin ensures a route for carbon export to the deep ocean (Whitney et al., 2005). Our results show, however, that the influence of mesoscale eddies does not extend homogeneously throughout the GOA. Haida eddies rarely propagate further west than $\sim 145^\circ\text{W}$, and Yakutat eddies rarely drift greater than ~ 250 km from the shelf break (Fig. 5), creating an ‘eddy desert’ where the probability of an eddy occurring is extremely low. Here, the HNLC conditions will rarely be alleviated by the passage of mesoscale eddies, which may contribute to the very low primary productivity and carbon export of the area.

This eddy census quantifies the interannual and spatial variability in the location and properties of anticyclonic eddies in the GOA. It is hoped the results will be valuable for cruise planning and to provide interannual and spatial context for *in situ* data. Future work will further investigate the forcing factors influencing the number and location of eddies, and their subsequent impact on biological populations.

Acknowledgements

This paper benefited from discussion with Steven Bograd and others at NOAA PFEL ERD. The altimeter products were produced by Ssalto/Duacs and distributed by Aviso, with support from CNES.

NCEP Reanalysis wind data were provided by the NOAA-CIRES Climate Diagnostics Center, Boulder, Colorado, USA. This work was funded by NSF grants OCE-0535386 and OCE-0531289 to ACT. This is contribution number 576 to the US GLOBEC program.

References

- Batten, S.D., Crawford, W.R., 2005. The influence of coastal origin eddies on oceanic plankton distributions in the eastern Gulf of Alaska. *Deep Sea Research Part II* 52 (7–8), 991–1010.
- Boyd, P.W., Law, C.S., Wong, C.S., Nojiri, Y., Tsuda, A., Lvasseur, M., Takeda, S., Rivkin, R., Harrison, P.J., Strzepak, R., Gower, J., McKay, R.M., Abraham, E.R., Arychuk, M., Barwell-Clarke, J., Crawford, W.R., Crawford, D., Hale, M., Harada, K., Johnson, K.S., Kiyosawa, H., Kudo, I., Marchetti, A., Miller, W., Needoba, J., Nishioka, J., Ogawa, H., Page, J., Robert, M., Saito, H., Sastri, A., Sherry, N., Soutar, T., Sutherland, N.E., Taira, Y., Whitney, F., Wong, S.K.E., Yoshimura, T., 2004. The decline and fate of an iron-induced subarctic phytoplankton bloom. *Nature* 428, 549–553.
- Chelton, D.B., Schlax, M.G., Samelson, R.M., de Szoeke, R.A., 2007. Global observations of large oceanic eddies. *Geophysical Research Letters* 34, L15606.
- Combes, V., Di Lorenzo, E., 2007. Intrinsic and forced interannual variability of the Gulf of Alaska mesoscale circulation. *Progress in Oceanography* 75, 266–286.
- Crawford, W.R., 2002. Physical characteristics of Haida eddies. *Journal of Oceanography* 58, 703–713.
- Crawford, W.R., 2005. Heat and freshwater transport by eddies into the Gulf of Alaska. *Deep Sea Research Part II* 52 (7–8), 893–908.
- Crawford, W.R., Whitney, F.A., 1999. Mesoscale eddy swirl with data in Gulf of Alaska. *EOS Transactions* 80 (33), 365–376.
- Crawford, W.R., Cherniawsky, J.Y., Foreman, M.G.G., 2000. Multi-year meanders and eddies in the Alaskan Stream as observed by TOPEX/Poseidon altimeter. *Geophysical Research Letters* 27 (7), 1025–1028.
- Crawford, W.R., Cherniawsky, J.Y., Foreman, M.G.G., Gower, J.F.R., 2002. Formation of the Haida-1998 oceanic eddy. *Journal of Geophysical Research—Oceans* 107 (C7), 3069.
- Crawford, W.R., Brickley, P.J., Peterson, T.D., Thomas, A.C., 2005. Impact of Haida eddies on chlorophyll distribution in the Eastern Gulf of Alaska. *Deep Sea Research Part II* 52 (7–8), 975–990.
- Crawford, W.R., Brickley, P.J., Thomas, A.C., 2007. Eddy transport into a cyclonic gyre: an example in the Gulf of Alaska. *Progress in Oceanography* 75, 287–303.
- Di Lorenzo, E., Foreman, M.G.G., Crawford, W.R., 2005. Modelling the generation of Haida eddies. *Deep Sea Research Part II* 52 (7–8), 853–874.
- Emery, W.J., Hamilton, K., 1985. Atmospheric forcing of interannual variability in the Northeast Pacific Ocean—connections with El Niño. *Journal of Geophysical Research—Oceans* 90 (NC1), 857–868.
- Gower, J.F.R., 1989. Geosat altimeter observations of the distribution and movement of sea-surface height anomalies in the north-east Pacific, in *Oceans 89: the global ocean*. Seattle IEEE pp. 977–981.
- Isern-Fontanet, J., Garcia-Ladona, E., Font, J., 2003. Identification of marine eddies from altimetric maps. *Journal of Atmospheric and Oceanic Technology* 20 (5), 772–778.
- Isern-Fontanet, J., Font, J., Garcia-Ladona, E., Emelianov, M., Millot, C., Taupier-Letage, I., 2004. Spatial structure of anticyclonic eddies in the Algerian Basin (Mediterranean Sea) analyzed using the Okubo–Weiss parameter. *Deep Sea Research Part II* 51 (25–26), 3009–3028.
- Isern-Fontanet, J., Garcia-Ladona, E., Font, J., 2006. Vortices of the Mediterranean Sea: an altimetric perspective. *Journal of Physical Oceanography* 36 (1), 87–103.
- Johnson, W.K., Miller, L.A., Sutherland, N.E., Wong, C.S., 2005. Iron transport by mesoscale Haida eddies in the Gulf of Alaska. *Deep Sea Research Part II* 52 (7–8), 933–954.
- Kirwan, A.D., McNally, G.J., Reyna, E., Merrell, W.J., 1978. Near-surface circulation of eastern North Pacific. *Journal of Physical Oceanography* 8 (6), 937–945.
- Ladd, C., 2007. Interannual variability of the Gulf of Alaska eddy field. *Geophysical Research Letters* 34, L11605.
- Ladd, C., Kachel, N.B., Mordy, C.W., Stabeno, P.J., 2005a. Observations from a Yakutat eddy in the northern Gulf of Alaska. *Journal of Geophysical Research—Oceans* 110 (C3), C03003.
- Ladd, C., Stabeno, P.J., Cokelet, E.D., 2005b. A note on cross-shelf exchange in the northern Gulf of Alaska. *Deep Sea Research Part II* 52 (5–6), 667–679.
- Ladd, C., Mordy, C.W., Kachel, N.B., Stabeno, P.J., 2007. Northern Gulf of Alaska eddies and associated anomalies. *Deep Sea Research Part I* 54, 487–509.
- Le Traon, P.Y., Faugere, Y., Hernandez, F., Dorandeu, J., Mertz, F., Ablain, M., 2003. Can we merge GEOSAT follow-on with TOPEX/Poseidon and ERS-2 for an improved description of the ocean circulation? *Journal of Atmospheric and Oceanic Technology* 20 (6), 889–895.
- Mackas, D.L., Galbraith, M.D., 2002. Zooplankton distribution and dynamics in a North Pacific eddy of coastal origin: 1. Transport and loss of continental margin species. *Journal of Oceanography* 58 (5), 725–738.
- Martin, J.H., Fitzwater, S., 1988. Iron deficiency limits phytoplankton growth in the Northeast Pacific subarctic. *Nature* 331 (6154), 341–343.
- Matthews, P.E., Johnson, M.A., O'Brien, J.J., 1992. Observation of mesoscale ocean features in the Northeast Pacific using Geosat radar altimetry data. *Journal of Geophysical Research—Oceans* 97 (C11), 17829–17840.
- Melsum, A., Meyers, S.D., Hurlburt, H.E., Metzger, J.E., O'Brien, J.J., 1999. ENSO effects on the Gulf of Alaska eddies. *Earth Interactions* 3, 1–30.
- Melsum, A., Metzger, J.E., Hurlburt, H.E., 2003. Impact of remote oceanic forcing on Gulf of Alaska sea levels and mesoscale circulation. *Journal of Geophysical Research—Oceans* 108 (C11), 3346.
- Miller, L.A., Robert, M., Crawford, W.R., 2005. The large, westward propagating Haida eddies of the Pacific eastern boundary. *Deep Sea Research Part II* 52 (7–8), 845–852.
- Murray, C.P., Morey, S.L., O'Brien, J.J., 2001. Interannual variability of upper ocean vorticity balances in the Gulf of

- Alaska. *Journal of Geophysical Research—Oceans* 106 (C3), 4479–4491.
- Musgrave, D.L., Weingartner, T.J., Royer, T.C., 1992. Circulation and hydrography in the northwestern Gulf of Alaska. *Deep Sea Research Part A* 39 (9A), 1499–1519.
- Okkonen, S.R., Jacobs, G.A., Metzger, J.E., Hurlburt, H.E., Shriver, J.F., 2001. Mesoscale variability in the boundary currents of the Alaska Gyre. *Continental Shelf Research* 21 (11–12), 1219–1236.
- Okkonen, S.R., Weingartner, T.J., Danielson, S.L., Musgrave, D.L., Schmidt, G.M., 2003. Satellite and hydrographic observations of eddy-induced shelf-slope exchange in the northwestern Gulf of Alaska. *Journal of Geophysical Research—Oceans* 108 (C2), 3033.
- Okubo, A., 1970. Horizontal dispersion of floatable particles in the vicinity of velocity singularity such as convergences. *Deep Sea Research* 17, 445–454.
- Pascual, A., Faugere, Y., Larnicol, G., Le Traon, P.Y., 2006. Improved description of the ocean mesoscale variability by combining four satellite altimeters. *Geophysical Research Letters* 33, L03611.
- Pasquero, C., Provenzale, A., Babiano, A., 2001. Parameterization of dispersion in two-dimensional turbulence. *Journal of Fluid Mechanics* 439, 279–303.
- Peterson, T.D., Whitney, F.A., Harrison, P.J., 2005. Macronutrient dynamics in an anticyclonic mesoscale eddy in the Gulf of Alaska. *Deep Sea Research Part II* 52 (7–8), 909–932.
- Reed, R.K., Schumacher, J.D., 1986. Physical oceanography, in the Gulf of Alaska: physical environment and biological resources. In: Hood, D.W., Zimmerman, S.T., (Eds.) *Minerals Management Service*, Springfield, pp. 57–75.
- Schwing, F.B., Murphree, T., deWitt, L., Green, P.M., 2002. The evolution of oceanic and atmospheric anomalies in the northeast Pacific during the El Niño and La Niña events of 1995–2001. *Progress in Oceanography* 54 (1–4), 459–491.
- Stabeno, P.J., Bond, N.A., Hermann, A.J., Kachel, N.B., Mordy, C.W., Overland, J.E., 2004. Meteorology and oceanography of the northern Gulf of Alaska. *Continental Shelf Research* 24 (7–8), 859–897.
- Stammer, D., 1997. Global characteristics of ocean variability estimated from regional TOPEX/Poseidon altimeter measurements. *Journal of Physical Oceanography* 35, 1650–1666.
- Swaters, G.E., Mysak, L.A., 1985. Topographically induced baroclinic eddies near a coastline, with application to the Northeast Pacific. *Journal of Physical Oceanography* 15 (11), 1470–1485.
- Tabata, S., 1982. The anticyclonic, baroclinic eddy off Sitka, Alaska in the Northeast Pacific Ocean. *Journal of Physical Oceanography* 12 (11), 1260–1282.
- Thomson, R.E., Gower, J.F.R., 1998. A basin-scale oceanic instability event in the Gulf of Alaska. *Journal of Geophysical Research—Oceans* 103 (C2), 3033–3040.
- Waugh, D.W., Abraham, E.R., Bowen, M.M., 2006. Spatial variations of stirring in the surface ocean: a case study of the Tasman Sea. *Journal of Physical Oceanography* 36 (3), 526–542.
- Weiss, J., 1991. The dynamics of enstrophy transfer in two-dimensional hydrodynamics. *Physica D* 48, 273–294.
- Whitney, F.A., Robert, M., 2002. Structure of Haida eddies and their transport of nutrient from coastal margins into the NE Pacific Ocean. *Journal of Oceanography* 58 (5), 715–723.
- Whitney, F.A., Crawford, W.R., Yoshimura, T., 2005. The uptake and export of silicon and nitrogen in HNLC waters of the NE Pacific Ocean. *Deep Sea Research Part II* 52 (7–8), 1055–1067.
- Willmott, A.J., Mysak, L.A., 1980. Atmospherically forced eddies in the Northeast Pacific. *Journal of Physical Oceanography* 10 (11), 1769–1791.
- Yelland, D., Crawford, W.R., 2005. Currents in Haida eddies. *Deep Sea Research Part II* 52, 875–892.